

Peptide-Based Trihydroxamates as Models for Desferrioxamines. Iron(III)-Holding Properties of Linear and Cyclic *N*-Hydroxy Peptides with an L-Alanyl-L-alanyl-*N*-hydroxy- β -alanyl Sequence

Yukihiro Hara and Masayasu Akiyama*

Department of Applied Chemistry, Tokyo University of Agriculture and Technology,
Koganei, Tokyo 184, Japan

Received October 18, 1995[⊗]

A pair of linear and cyclic peptide-based trihydroxamate ligands (**1** and **2**) have been prepared through fragment condensation of suitably protected Ala-Ala- β (HO)Ala units. These ligands have an eight-atom spacing between hydroxamic acid groups and compare in chain length with natural desferrioxamines of a nine-atom spacing. Ligands **1** and **2** form hexadentate octahedral complexes with iron(III), Fe(III)-**1** and Fe(III)-**2**, in aqueous solution. The complexes show absorptions at λ_{max} 425 nm with ϵ ca. 2800, characteristic of a 1:3 iron(III) complex with a hydroxamate group. Absorption vs pH profiles give ranges of pH 4–9.5 and 6.7–8.7 for Fe(III)-**1** and Fe(III)-**2**, respectively, where each of them exists as the 1:3 complex. The ligand protonation constants ($\text{p}K_1$, $\text{p}K_2$, $\text{p}K_3$) are determined, and the stability constants [10^{27} for Fe(III)-**1** and 10^{28} for Fe(III)-**2**] obtained are rather close to values of 10^{30} s for ferrioxamines. However, the absorption vs pH profile for the complexes and their iron(III)-exchange kinetics with EDTA show that the iron(III)-holding capacity of these complexes is still lower than that of ferrioxamine B. The kinetic data indicate that Fe(III)-**2** holds iron more tightly than Fe(III)-**1**. The alanine residues exert their chiral influence on the coordination. Fe(III)-**1** and Fe(III)-**2** reveal large negative and positive Cotton effects at 445 and 360 nm in their CD spectra, showing that the complexes are preferentially in the Δ configuration around the metal ion. Thus, it is concluded that the Ala-Ala- β (HO)Ala sequence is a useful unit for making chiral ligands which form stable iron(III) complexes of well-defined structure.

Introduction

Siderophores are naturally occurring, low-molecular-weight, iron(III)-chelating compounds produced by microorganisms under iron-deficient conditions. These compounds generally contain three bidentate groups of either hydroxamate or catecholate type in linear, cyclic, or tripodal arrangements and form stable octahedral complexes with iron(III) in order to solubilize otherwise insoluble ferric oxides. Microorganisms take up iron(III) as siderophore complexes and transport it into their cells via membrane receptors.^{1–7} Siderophore-mediated, microbial iron assimilation involves various chemical processes which are related to fundamental questions regarding iron coordination and molecular recognition. This fact has stimulated considerable interest in the design and synthesis of artificial siderophores.^{8–11}

Among naturally abundant hydroxamate siderophores, the class of ferrioxamines (A–G varieties) occur as stable iron(III)

complexes of linear and cyclic trihydroxamates.² Desferrioxamine B is used currently as the drug of choice for treatment of iron-overloaded patients, although its limitations have prompted an extensive search for economically and therapeutically more useful iron(III)-chelating compounds.¹² As part of this research, effort has been directed toward the synthesis or fermentative preparation of biomimetic desferrioxamines.^{13–16} Of great interest is the synthesis of peptide-based trihydroxamates, since these derivatives can be designed on the basis of peptide structure. Furthermore, peptides themselves constitute a rich source of useful information regarding structure–property and structure–function relationships. Desferrioxamine-like trihydroxamates can be obtained as sequential peptides by joining suitable *N*-hydroxy peptide segments, and a few of tris-(*N*-hydroxy peptides) have already been prepared from α -amino acid units.^{16–18} A previous paper described the synthesis of a nonapeptide trihydroxamic acid with an Ala-(HO)Gly-Ala¹⁹

[⊗] Abstract published in *Advance ACS Abstracts*, August 1, 1996.

- (1) Winkelmann, G., Ed. *Handbook of Microbial Iron Chelates*; CRC Press: Boca Raton, FL, 1991.
- (2) Keller-Schierlein, W.; Prelog, V.; Zähler, H. *Fortschr. Chem. Org. Naturst.* **1964**, *22*, 279.
- (3) Neilands, J. B. *Science* **1967**, *156*, 1443; *Struct. Bonding* **1984**, *58*, 1.
- (4) Emery, T. In *Metal Ions in Biological Systems*; Sigel, H., Ed.; Marcel Dekker: New York, 1978; Vol. 7, Chapter 3.
- (5) (a) Raymond, K. N.; Müller, G.; Matzanke, B. F. *Top. Curr. Chem.* **1984**, *123*, 49. (b) Matzanke, B. F.; Müller-Matzanke, G.; Raymond, K. N. In *Iron Carriers and Iron Proteins*; Loehr, T. M., Ed.; Physical Bioinorganic Chemistry Series, Vol. 5; VCH Publishers: New York, 1989; Chapter 1.
- (6) Hider, R. C. *Struct. Bonding* **1984**, *58*, 25.
- (7) Braun, V.; Winkelmann, G. *Prog. Clin. Biochem. Med.* **1987**, *5*, 67.
- (8) Hou, Z.; Whisenhunt, D. W., Jr.; Xu, J.; Raymond, K. N. *J. Am. Chem. Soc.* **1994**, *116*, 840. Loomis, L. D.; Raymond, K. N. *Inorg. Chem.* **1991**, *30*, 906. Raymond, K. N.; Carrano, J. C. *Acc. Chem. Res.* **1979**, *12*, 183.
- (9) Dayan, I.; Libman, J.; Agi, Y.; Shanzer, A. *Inorg. Chem.* **1993**, *32*, 1467. Tor, Y.; Libman, J.; Shanzer, A.; Felder, C. E.; Lifson, S. J. *Am. Chem. Soc.* **1992**, *114*, 6661.

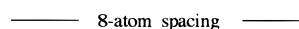
- (10) Akiyama, M.; Katoh, A.; Kato, J.; Takahashi, K.; Hattori, K. *Chem. Lett.* **1991**, 1189. Akiyama, M.; Katoh, A.; Mutoh, T. *J. Org. Chem.* **1988**, *53*, 6089.
- (11) Esteves, M. A.; Vaz, M. C. T.; Gonçalves, M. L. S. S.; Farkas, E.; Santos, M. A. *J. Chem. Soc., Dalton Trans.* **1995**, 2565.
- (12) (a) Bergeron, R. J.; Brittenham, G. M., Eds. *The Development of Iron Chelators for Clinical Use*; CRC Press: Boca Raton, FL, 1994. (b) Martell, A. E.; Anderson, W. F.; Badman, D. G., Eds. *Development of Iron Chelators for Clinical Use*; Elsevier/North Holland: New York, 1981.
- (13) Shimizu, K.; Akiyama, M. *J. Chem. Soc., Chem. Commun.* **1985**, 183.
- (14) Shimizu, K.; Nakayama, K.; Akiyama, M. *Bull. Chem. Soc. Jpn.* **1986**, *59*, 2421.
- (15) Konetshny-Rapp, S.; Jung, G.; Raymond, K. N.; Meiwes, J.; Zähler, H. *J. Am. Chem. Soc.* **1992**, *114*, 2224.
- (16) Yakirevitch, P.; Rochel, N.; Albrecht-Gary, A. M.; Libman, J.; Shanzer, A. *Inorg. Chem.* **1993**, *32*, 1779.
- (17) Shimizu, K.; Nakayama, K.; Akiyama, M. *Bull. Chem. Soc. Jpn.* **1984**, *57*, 2456.
- (18) Akiyama, M.; Katoh, A.; Iijima, M.; Takagi, T.; Natori, K.; Kojima, T. *Bull. Chem. Soc. Jpn.* **1992**, *65*, 1356.

sequence, together with the formation of its octahedral chiral iron complex.¹⁸ As indicated by its low stability constant and weak CD intensity, the complex was not sufficiently stable or isomerically pure, owing to a chain constraint caused by a short distance between the hydroxamate groups.¹⁸ In order to provide more useful iron(III) chelates, we have modified the nonapeptide sequence. This paper reports the iron(III)-holding properties of a pair of linear and cyclic trihydroxamic acids prepared from a new tripeptide sequence. This sequence appears to be useful for making chiral ligands which produce stable iron(III) complexes of well-defined structure.

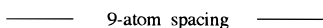
Results and Discussion

Unit Sequence. Replacement of the (HO)Gly residue in the previous nonapeptide by a β (HO)Ala residue¹³ was expected to afford a better ligand for sequestration of iron(III). A monohydroxamate segment, an Ala-Ala- β (HO)Ala sequence, will give a trihydroxamate ligand having an eight-atom spacing with two amide bonds between the hydroxamic acid groups (sequence 1). The ligand is larger by three atoms than the nonapeptide and compares in chain length with desferrioxamines² which have a nine-atom spacing carrying pentamethylene and ethylene units with one amide bond (sequence 2). In

Sequence 1: $-\text{CON}(\text{OH})-\text{[CH}_2\text{CH}_2\text{CONHCHMeCONHCHMe]}-\text{CON}(\text{OH})-$



Sequence 2: $-\text{CON}(\text{OH})-\text{[CH}_2\text{CH}_2\text{CH}_2\text{CH}_2\text{CH}_2\text{NHCOCCH}_2\text{CH}_2\text{]}-\text{CON}(\text{OH})-$

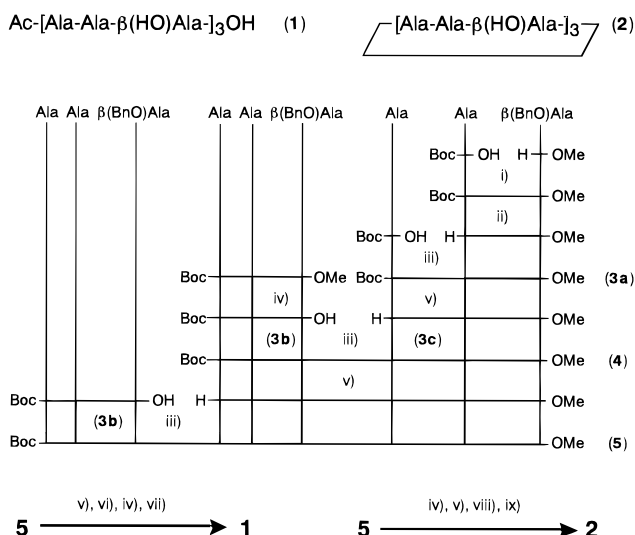


comparison with desferrioxamines, the present ligand is relatively constrained; its component sequence is short one atom yet has one more amide bond. This constraint, however, favors chiral complex formation by forcing tight coordination of ligating groups to the metal ion, although it may also affect stabilization of the resulting complex.

Synthesis. The synthetic procedure is depicted in Scheme 1. The Boc (*t*-BuO-CO-) group was used to protect the amino group during the synthesis and then replaced by the acetyl group. The methyl group was used for protection of the carboxyl group. Methyl 3-((benzyloxy)amino)propanoate was acylated by the mixed-anhydride method, while other coupling reactions were performed by a racemization-saving carbodiimide method.²⁰ Fragment condensations of the protected Ala-Ala- β (BnO)Ala units produced the protected di- and trihydroxamate derivatives in good yields, and the linear derivative was cyclized with a (benzotriazolyl)phosphonium (BOP) reagent²¹ under high dilution conditions. The molecular size of the cyclization product was estimated by the GPC method. Catalytic hydrogenation removed the benzyl protective groups to afford the final products, linear and cyclic ligands (**1** and **2**), which were characterized by HPLC, IR, ¹H NMR, and elemental analysis.

NMR Spectroscopy. ¹H NMR data were obtained in DMSO-*d*₆ solution. Spectral signals were assigned with the aid of decoupling experiments and are listed in Table 1. For both

Scheme 1^a



^a Reagents: (i) Cl-CO₂Buⁱ/Et₃N; (ii) 9 mol dm⁻³ HCl/dioxane, 0 °C; (iii) EDC/HOBt; (iv) 1 mol dm⁻³ NaOH/MeOH; (v) TFA, 0 °C; (vi) AcOSu; (vii) H₂-Pd(OAc)₂; (viii) BOP/HOBt/NMM; (ix) H₂-Pd/C.

Table 1. ¹H NMR Spectral Data for Ligands **1** and **2**^a

assignt	linear 1			cyclic 2		
	δ_{H} /ppm	<i>J</i> /Hz	Tc ^b / ppb deg ⁻¹	δ_{H} /ppm	<i>J</i> /Hz	Tc ^b / ppb deg ⁻¹
CH ₃ (Ala ¹)	1.16 (d)	6.4		1.16 (d)	7.0	
CH ₃ (Ala ²)	1.19 (d)	6.4		1.19 (d)	7.0	
CH ₃ (Ac)	1.83 (s)					
NCH ₂ CH ₂ CO	2.39 (t)	7.1		2.41 (m)		
NCH ₂ CH ₂ CO	3.68 (m)			3.73 (m)		
CH (Ala ¹)	4.30 (qn)	6.4		4.25 (qn)	7.2	
CH (Ala ²)	4.76 (qn)	7.3		4.76 (qn)	6.8	
NH (Ala ² × 1)	7.85 (d)	7.8	-5.2			
NH (Ala ²)	7.89 (d)	7.8	-5.2	7.77 (d)	4.9	-4.3
NH (AcAla ¹)	8.00 (d)	7.8	-4.0			
NH (Ala ¹)	8.11 (d)	7.8	-4.0	8.07 (d)	7.0	-1.8
N-OH	9.93 (s)			10.03 (s)		

^a 270 MHz in DMSO-*d*₆ at 25 °C. The sequence for the assignment is as follows: Ac-[Ala¹-Ala²-N(OH)CH₂CH₂CO-]₃-OH. Sample concentrations: **1**, 15 mmol dm⁻³; **2**, 20 mmol dm⁻³. qn = quintet. ^b Tc: a temperature coefficient for amide proton chemical shifts between 25 and 50 °C in ppb (ppm × 10⁻³).

ligands **1** and **2**, the α -proton of the Ala-*N*-OH residue appeared at δ 4.76 ppm¹⁸ as a quintet with the expected intensity, which confirmed the full presence of the hydroxamate groups in the ligands. Cyclic ligand **2** revealed a C₃-symmetric spectral pattern and showed the presence of one set of intramolecularly hydrogen-bonded amide protons,²² as exhibited by a small value of the temperature coefficient for the β (OH)Ala-NH resonance. No such proton was observed for linear ligand **1**; thus ligand **1** is considered to remain rather free in a polar solvent like DMSO, with its amide groups exposed to the solvent. As an examination of the corresponding CPK molecular model suggests, the intramolecular hydrogen bonds of ligand **2** are reasonably accommodated in a conformation with the hydroxamate groups projecting outward from the ring (Figure 1). Iron(III) complex formation requires inward orientation of the hydroxamate groups; therefore, no precise preorganization for complexation²³ is provided by ligands **1** and **2**.

Iron(III) Complex Formation. An iron(III) complex was produced through a sequential procedure in aqueous solution.

(19) Abbreviations are as follows: Ala, L-alanine; β (HO)Ala or β (BnO)Ala, *N*-hydroxy- or *N*-(benzyloxy)- β -alanine; (HO)Gly, *N*-hydroxyglycine; Boc, *tert*-butoxycarbonyl; BOP, (benzotriazol-1-yloxy)tris(dimethylamino)phosphonium hexafluorophosphate(V); dien, diethylenetriamine; EDC, 1-ethyl-3-[3-(dimethylamino)propyl]carbodiimide; HOBt, 1-hydroxybenzotriazole; NMM, *N*-methylmorpholine; TFA, trifluoroacetic acid; AcOSu, *N*-acetoxysuccinimide; THF, tetrahydrofuran; DMSO, dimethyl sulfoxide; GPC, gel permeation chromatography

(20) König, W.; Geiger, R. *Chem. Ber.* **1970**, *103*, 788.

(21) Castro, B.; Dormoy, J. R.; Evin, G.; Selve, C. *Tetrahedron Lett.* **1975**, *1222*.

(22) The insolubility of the ligand in CH₂Cl₂, CHCl₃, and CH₃CN precluded a solution IR study for the presence of hydrogen bonds.

(23) Cram, D. J. *Science* **1988**, *240*, 760.

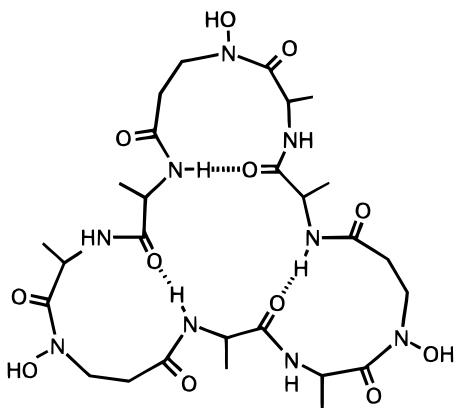


Figure 1. Possible conformation for intramolecularly hydrogen-bonded cyclic ligand **2**.

Table 2. Iron(III) Complex Formation and Protonation Equilibrium Data from Schwarzenbach Plots^a

complex	$\lambda_{\max}/\text{nm} (\epsilon)^b$		$K_{\text{Fe(HL)}}^c$	pH ^c	$\epsilon_{\text{Fe(HL)}}^d$
	pH 2.1	pH 7.0			
Fe(III)-1	465 (1860)	425 (2890)	1.44×10^3	3.2	(1960)
Fe(III)-2	465 (1720)	425 (2830)	4.14×10^4	4.6	(1930)
iron(III) nonapeptide ^e	450 (1650)	410 (2160)	2.24×10^6	6.4	(1760)

^a Determined in water at 25.0 ± 0.1 °C. ^b Values of $\epsilon/\text{dm}^3 \text{mol}^{-1} \text{cm}^{-1}$ are given in parentheses. ^c Half-protonation pH from the $K_{\text{Fe(HL)}}$ value. ^d ϵ at 425 or 410 nm. ^e Reference 18.

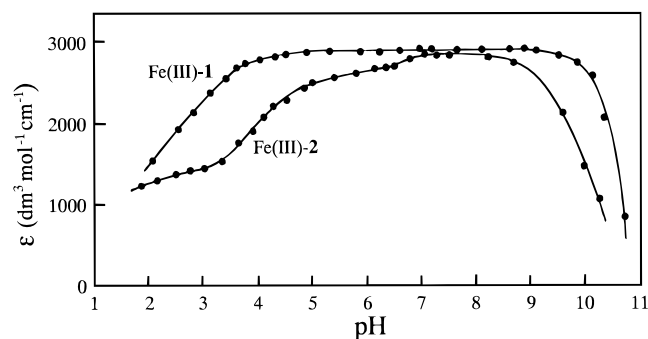


Figure 2. Absorption vs pH plots. Values of $\epsilon/\text{dm}^3 \text{mol}^{-1} \text{cm}^{-1}$ at 425 nm in water at 25.0 °C for Fe(III)-1 and Fe(III)-2 are plotted against pH.

Mixing of a slight excess (3 mol %) of ligand **1** or **2** with $\text{Fe}(\text{NO}_3)_3$ in water gave a solution of pH 2.1, which contained essentially a 1:2 complex of iron(III) with a hydroxamate group, a diaquobis(hydroxamato)iron(III) species.^{24,25} The 1:2 complex was smoothly transformed into a 1:3 complex by gradual neutralization with aqueous NaOH. The 1:3 complex [Fe(III)-1 or Fe(III)-2] showed its characteristic absorption at λ_{\max} 425 nm with ϵ ca. $2800 \text{ dm}^3 \text{mol}^{-1} \text{cm}^{-1}$ ²⁶ (Table 2).

Iron(III) Complexes in Water. Using electronic spectroscopy, the stability of iron(III) complexes against H^+ or OH^- attack can be estimated from the span of a top plateau region in a plot of ϵ (at 425 nm) vs pH (Figure 2). Fe(III)-1 has a constant region over pH 4.0–9.5 which is much wider than that (pH 6.5–8.5) of the previous nonapeptide.¹⁸ Fe(III)-2 reveals a top constant region (pH 6.7–8.7) with a lower, flat region (pH 4.7–6.7), the latter corresponding to an overlapping region where both 1:3 and 1:2 complexes coexist, as analyzed by a

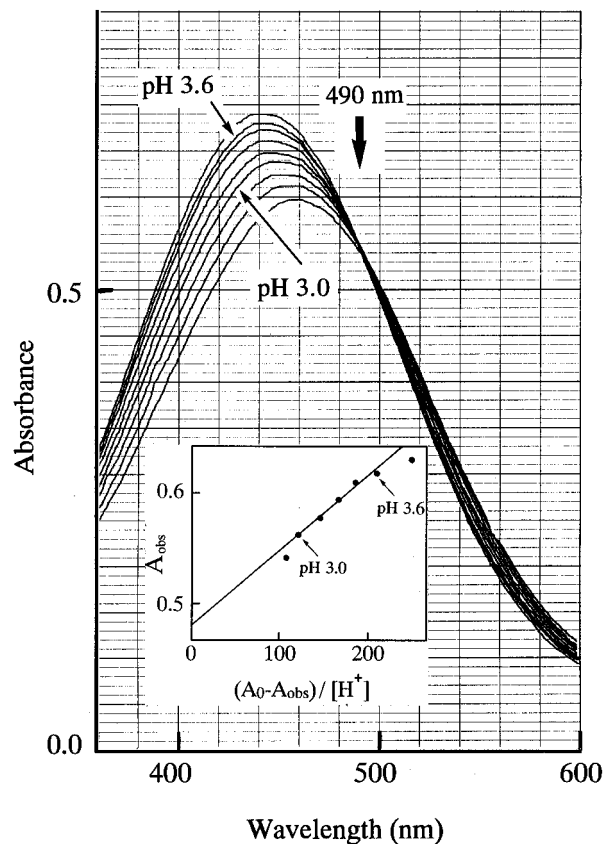


Figure 3. UV-visible spectra of Fe(III)-1 ($2.62 \times 10^{-4} \text{ mol dm}^{-3}$) in the range pH 2.7–3.8 in water at 25.0 °C. The insert is a Schwarzenbach plot for the range pH 3.0–3.6.

protonation equilibrium. The narrow top region for Fe(III)-2 indicates that there is a significant strain in the cyclic ligand; the strain requires a progressive dissociation of the hydroxamate groups to coordinate to iron(III), whereas the produced 1:3 complex can survive only at a low OH^- concentration.

As the pH was lowered from the region of a 1:3 complex, λ_{\max} shifted to a longer wavelength and the ϵ value decreased. Fe(III)-1 gave an isosbestic point at 490 nm over a range of pH 2.7–3.8 (Figure 3), indicating the presence of an equilibrium between a 1:3 complex (Fe(L)) and its protonated species (Fe(HL)⁺), as expressed by eqs 1 and 2. (Similarly, the spectrum



$$K_{\text{Fe(HL)}} = [\text{Fe(HL)}^+]/[\text{H}^+][\text{Fe(L)}] \quad (2)$$

$$A_{\text{obs}} = (A_{\text{Fe(L)}} - A_{\text{obs}})/[\text{H}^+]K_{\text{Fe(HL)}} + \epsilon_{\text{Fe(HL)}}c_{\text{total}} \quad (3)$$

of Fe(III)-2 exhibited an isosbestic point at 485 nm.) This equilibrium may be described using the Schwarzenbach equation (3).²⁴ These spectral data were analyzed in terms of eq 3, as shown for the case of Fe(III)-1 (an insert of Figure 3). The protonation equilibrium data are included in Table 2. A log $K_{\text{Fe(HL)}}$ value (a half-protonation pH) is an estimate of the ease with which a 1:3 complex can be formed in competition with protonation. Fe(III)-2 or Fe(III)-1 is stable to a lower pH region than the iron(III) nonapeptide (Table 2) due to its lower chain strain. This indicates that chain flexibility is a major factor controlling the stability of the octahedral coordination. In this context, ferrioxamines, containing multiple CH_2 groups, are remarkably resistant to protonation, and cyclic ferrioxamine E is more resistant than linear ferrioxamine D₁ (stable to pH 0 vs pH 0.5).²⁶ Thus, the present constrained ligand case is in contrast to the ferrioxamine case.

(24) Schwarzenbach, G.; Schwarzenbach, K. *Helv. Chim. Acta* **1963**, *46*, 1390.

(25) Caudle, M. T.; Stevens, R. D.; Crumbliss, A. L. *Inorg. Chem.* **1994**, *33*, 843, and 6111.

(26) Anderegg, G.; L'Epplattenier, F.; Schwarzenbach, G. *Helv. Chim. Acta* **1963**, *46*, 1400, 1409.

Table 3. Ligand Protonation Constants and Iron Complex Stability Constants^a

ligand	pK ₁	pK ₂	pK ₃	pK _{av} ^b	log K _{Fe(L)}
1	9.73	9.10	8.65	9.18	27.4
2	10.03	9.23	8.54	9.27	28.3
DFD ₁ ^c	9.69	9.24	8.50	9.14	30.8
D ₁ ^d	10.03	9.24	8.65	9.32	32.2

^a Values for pK's were determined in water at 25.0 ± 0.1 °C with ionic strength 0.01 (KCl), and those of log K_{Fe(L)} are derived from the data determined at an ionic strength of 0.10 in Table 4; similar values for log K_{Fe(L)} were obtained at ionic strength 0.01. ^b pK_{av} = 1/3(pK₁ + pK₂ + pK₃). ^c DFD₁ = N-acetylated desferrioxamine B; ref 26. ^d D₁ = desferrioxamine E; ref 15.

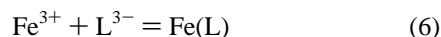
Protonation and Stability Constants. The protonation constants for a trihydroxamic acid (H₃L) such as ligand **1** or **2** are defined by the generalized equations (4) and (5), where *n*



$$K_n = [\text{H}_n\text{L}^{n-3}]/[\text{H}^+][\text{H}_{n-1}\text{L}^{n-4}] \quad (5)$$

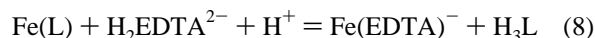
= 1, 2, or 3. Ligands **1** and **2** were soluble in water, a trait desirable for siderophore models.⁶ Potentiometric titration experiments were carried out in water with 0.1 mol dm⁻³ NaOH solution at 25.0 ± 0.1 °C and with ionic strength 0.01 (KCl). The titration data were analyzed by the program PKAS²⁷ giving the protonation constants (pK_{*n*}); from these constants an average value (pK_{av}) is calculated (Table 3). The constants are comparable with those of the corresponding linear and cyclic desferrioxamines, D₁ (which is N-acetylated desferrioxamine B) and E.²⁶

The proton-independent stability constant (K_{Fe(L)}) for an iron(III) complex is defined by eqs 6 and 7. In order to obtain the



$$K_{\text{Fe(L)}} = [\text{Fe(L)}]/[\text{Fe}^{3+}][\text{L}^{3-}] \quad (7)$$

stability constant of these ligands, we carried out the ligand-exchange reaction of eq 8 using equimolar amounts of Fe(L)



and H₂EDTA²⁻ at 25.0 ± 0.1 °C, ionic strength 0.10 (KCl), and pH 7.0. At this pH, both Fe(III)-**1** and Fe(III)-**2** exist entirely as the 1:3 iron(III) complexes. An equilibrium quotient (K_{eq}) for eq 8 may be expressed using eq 9. This K_{eq} value is

$$K_{\text{eq}} = [\text{Fe(EDTA)}^-][\text{H}_3\text{L}]/[\text{Fe(L)}][\text{H}_2\text{EDTA}^{2-}][\text{H}^+] \quad (9)$$

calculated from the pH of the solution and the remaining [Fe(L)] and [H₂EDTA²⁻] and the produced [Fe(EDTA)] and [H₃L] by considering the dissociation of the species involved and the mass balance stoichiometry of eq 8. Equation 9 may be rearranged to give eq 10, using the following relations: [H₃L]

$$K_{\text{Fe(L)}} = (K_{\text{Fe(EDTA)}}/K_{\text{eq}})(K_1K_2K_3/K_1^{\text{edta}}K_2^{\text{edta}}) \quad (10)$$

= K₁K₂K₃[L³⁻][H³⁺] and [H₂EDTA²⁻] = K₁^{edta}K₂^{edta}[EDTA⁴⁻][H²⁺]. The stability constant (K_{Fe(L)}) is obtained from the K_{eq} value, the stability constant of Fe(III)-EDTA (K_{Fe(EDTA)}),²⁸ and the protonation constants of the ligand (K₁,

(27) Martell, A. E.; Motekaitis, R. J. *Determination and Use of Stability Constants*; VCH Publishers: New York, 1992.

(28) (a) Schwarzenbach, G.; Heller, J. *Helv. Chim. Acta* **1951**, *34*, 576. (b) Schwarzenbach, G.; Ackermann, H. *Helv. Chim. Acta* **1947**, *30*, 1798.

Table 4. Rate and Equilibrium Data for Iron(III)-Exchange Reactions at 25.0 °C and Ionic Strength 0.1

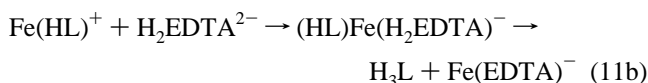
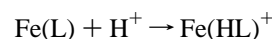
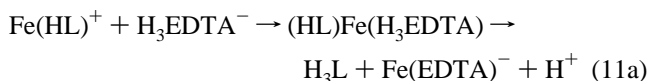
iron(III) complex	pH	exchange rate: ^a		competition equilibrium ^b	
		k _{obs} /s ⁻¹	% unexchanged	K _{eq} value	
Fe(III)- 1	2.1	3.2 × 10 ⁻¹	0.4	25	4.9 × 10 ⁸
	5.4	1.8 × 10 ⁻²			
	7.0				
Fe(III)- 2	2.1	1.0 × 10 ⁻¹	9.1	39	1.3 × 10 ⁸
	5.4	4.4 × 10 ⁻³			
	7.0				
ferrioxamine B	2.1	9.0 × 10 ⁻³	7.1 × 10 ^{-5 c}		
	5.3				

^a Buffers: glycine-HCl, pH 2.1; acetate-NaOH, pH 5.4. A 20 molar excess of EDTA was used for a given iron(III) complex (1.3 × 10⁻⁴ mol dm⁻³). ^b An equimolar competition reaction with EDTA (2.6 × 10⁻⁴ mol dm⁻³) was performed at the indicated pH without buffer. ^c Reference 13; here a 28 molar excess of EDTA was used.

K₂, and K₃) and EDTA (K₁^{edta} = 10.26 and K₂^{edta} = 6.16).²⁸ The values of log K_{Fe(L)} are listed in Table 3, and the equilibrium data are included in Table 4.

The stability constants for the two complexes are much larger than the 10¹⁷ value reported for the iron(III) nonapeptide.¹⁸ The stability constant for Fe(III)-**2** (10^{28.3}) is slightly larger than that for Fe(III)-**1** (10^{27.4}), probably due to its stronger iron-holding capacity and higher protonation constants. It is worthy of note that the stability constants for the present complexes, despite the constraint of the ligands, are nearly comparable with those (10³⁰ and 10³²) of ferrioxamines D₁ and E²⁶ and also with those (~10³²) of the cyclic fermentation products.¹⁵

Iron-Exchange Reactions. The iron(III)-holding capacity of a trihydroxamate ligand may be assessed using ligand-exchange reactions.²⁹ A reaction of this type was carried out using excess EDTA in water, as shown by eqs 11a and 11b for



reactions at pH 2.1 and 5.4, respectively, and the results are shown in Table 4 and Figure 4. It was found that Fe(III)-**2** exchanged iron(III) more slowly than Fe(III)-**1** at both pH 2.1 and 5.4 and that a rate acceleration factor with increasing proton concentration (for the rates at pH 2.1 vs pH 5.4) was small for Fe(III)-**1** (18-fold) and Fe(III)-**2** (23-fold), compared to that (124-fold) for ferrioxamine B. Additional kinetic experiments with Fe(III)-**1** revealed a hyperbolic dependence of the rate on the EDTA concentration at both pH 2.1 and 5.4 (Figure 4). In light of these results, a detailed consideration of the pathway is merited.

A general mechanism for metal ion exchanges between multidentate ligands has been formulated by Margerum and co-workers. An example is the reaction of (dien)₂Ni²⁺ with EDTA;³⁰ it involves an initial, slow, proton-assisted dissociation of one dien with the concomitant formation of a (aquo)₃Ni²⁺-(dien) species, followed by fast attack by EDTA to produce a mixed ternary complex. Tufano and Raymond reported iron(III)-exchange reactions between ferrioxamine B and EDTA which proceed by a similar mechanism involving an initial

(29) Crumbliss, A. L. In *Handbook of Microbial Iron Chelates*; Winkelmann, G., Ed.; CRC Press: Boca Raton, FL, 1991; Chapter 7.

(30) Margerum, D. W.; Rosen, H. M. *Inorg. Chem.* **1968**, *7*, 299.

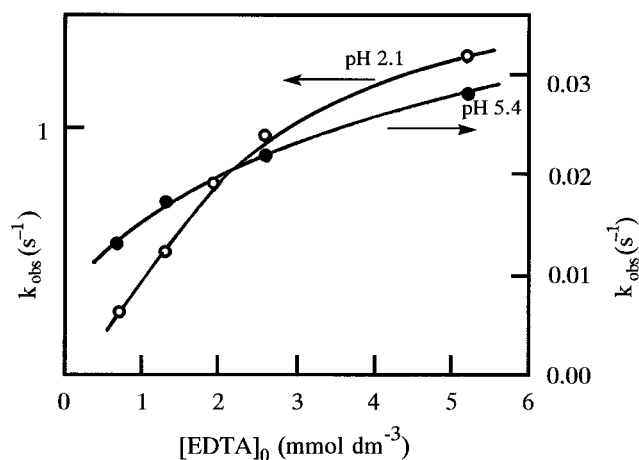


Figure 4. Dependence of the iron exchange rates of Fe(III)-1 on EDTA concentration at pH 2.1 (at 10.0 °C) (○) and at pH 5.4 (at 25.0 °C) (●). $[\text{Fe(III)-1}] = 1.3 \times 10^{-4} \text{ mol dm}^{-3}$.

proton-assisted pathway and the subsequent rate-determining ternary complex formation.³¹ In a similar exchange reaction, data reported by Albrecht-Gary et al. implicated the dissociation from the ternary complex to be the rate-determining step, although the authors could not specify which among the three groups dissociates at that step.³²

At pH 2.1, a diaquo(bis(hydroxamato)iron(III) species^{24,25} $[(\text{H}_2\text{O})_2\text{Fe}(\text{HL})]^+$ predominates for Fe(III)-1 and Fe(III)-2, as the data in Table 2 show. EDTA attacks this species directly, forming a ternary complex $[(\text{HL})\text{Fe}(\text{H}_3\text{EDTA})]$ and finally giving $\text{Fe}(\text{EDTA})^-$ even at this low pH.²⁸ There is a substantial difference in rates between Fe(III)-1 and Fe(III)-2; therefore, the rate-determining step does not occur at the stage of the initial attack by EDTA which is rapid and indiscriminate. This is supported by the hyperbolic dependence of the rate on the EDTA concentration, which indicates that the rate-determining step is preceded by EDTA addition.³² Therefore, the rate-determining step must be the transformation of the bis(hydroxamato)iron complex $[(\text{HL})\text{Fe}(\text{H}_3\text{EDTA})]$ into a mono(hydroxamato)iron complex $[(\text{H}_2\text{L})\text{Fe}(\text{HEDTA})]$, involving the dissociation of the second hydroxamato group.

At pH 5.4, Fe(III)-1 is not protonated, whereas some portion of Fe(III)-2 is protonated. According to the general mechanism, protonation of the complex should facilitate the attack of EDTA, leading to the transition state; hence the exchange reaction would be faster for Fe(III)-2 than for Fe(III)-1. We do not observe this result. Furthermore, a hyperbolic dependence of the rate on the EDTA concentration indicates that the association step with EDTA is followed by the rate-determining step.³² Therefore, it is more probable that, when the initial ternary complex is formed as $(\text{HL})\text{Fe}(\text{H}_2\text{EDTA})^-$, the iron(III) remains unexchanged; the leaving ligand can still hold the metal ion by the remaining two hydroxamato groups. The transition state of the reaction should occur at a stage where the second hydroxamato group is expelled by the incoming ligand, as in the reaction at pH 2.1. Thus, we propose this mechanism for the iron exchange in these peptide-based ligands. CPK molecular models of the two-hydroxamate binding show that the cyclic ligand may hold iron(III) more tightly, with its closed chain, than the linear ligand. It is seen here that an exchange reaction may indicate a result different from the protonation behavior in terms of previous models; in the former we observe that iron(III) is completely removed from the ligand, whereas in the latter it still remains in the ligand as partially aquated iron(III). What

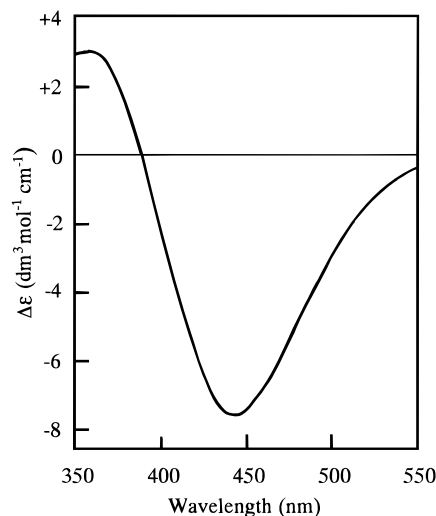


Figure 5. CD spectrum for Fe(III)-1: $\Delta\epsilon$ vs λ/nm in water at pH 7.0.

Table 5. Summary of CD Spectral Data in Water at Neutral pH

iron(III) complex	band/nm($\Delta\epsilon$)		type	ref
Fe(III)-1	360 (+3.0)	445 (-7.5)	Δ	
Fe(III)-2	360 (+4.4)	445 (-6.8)	Δ	
iron(III) nonapeptide	355 (+0.8)	435 (-1.8)	Δ	18
ferrichrome	360 (-3.7)	465 (+2.4)	Δ	35
coprogen	375 (+2.1)	474 (-1.3)	Δ	36

the acidic region of Figure 2 actually shows is that Fe(III)-2 is only more susceptible to protonation than Fe(III)-1.

Crumbliss's and Pribanic's groups studied the stepwise dissociation of iron(III) from ferrioxamine B in aqueous acid solution and specified the steps of dissociation of the first, second, and third hydroxamato groups to be fast, slow, and very slow, respectively.^{33,34} This stepwise dissociation suggests that the leaving of the third hydroxamato group might become the rate-determining step for the exchange reaction. However, in that case, almost throughout the exchange reaction the iron(III) ion is held in a hexacoordinated state by both entering and leaving ligands, and proton-assisted dissociation occurs easily even for the third hydroxamato group. That is, the state of the metal ion in this kind of exchange reaction is not the same as in a ligand dissociation reaction.

The rate constants at pH ca. 5.4 show that the iron(III)-holding capacity of desferrioxamine B outweighs the present ligands; ferrioxamine B resists H^+ attack more effectively due to its chain flexibility, and hence it becomes less susceptible to the proton-assisted iron(III)-exchange reaction. As the solution becomes acidic, however, the rate accelerates to a greater extent for ferrioxamine B than for the complexes of peptide ligands. This is likely due to a difference in the conformational flexibility. The peptide ligands are rigid to hold the bis(hydroxamato)iron(III) species transiently relative to desferrioxamine B.

Chirality of Complexes. Alanine residues exert their chiral influence during iron(III) complexation, as was the case with the nonapeptide.¹⁸ This influence is even more evident in the present case. The circular dichroism (CD) spectra of Fe(III)-1 and Fe(III)-2 exhibit large Cotton effects with negative (445 nm) and positive (360 nm) bands, as shown for Fe(III)-1 (Figure 5), where both intensities are much greater than that of the iron(III) nonapeptide (Table 5). Notably, their CD intensities exceed those of the well-defined, hydroxamate-type natural iron(III)

(31) Tufano, T. P.; Raymond, K. N. *J. Am. Chem. Soc.* **1981**, *103*, 6617.
 (32) Albrecht-Gary, A. M.; Palanche-Passeron, T.; Rochel, N.; Hennard, C.; Abdallah, M. A. *New J. Chem.* **1995**, *19*, 105.

(33) Monzyk, B.; Crumbliss, A. L. *J. Am. Chem. Soc.* **1982**, *104*, 4921.
 (34) Biruš, M.; Bradić, Z.; Krznarić, G.; Kujundžić, N.; Pribanić, M.; Wilkins, P. C.; Wilkins, R. G. *Inorg. Chem.* **1987**, *26*, 1000.

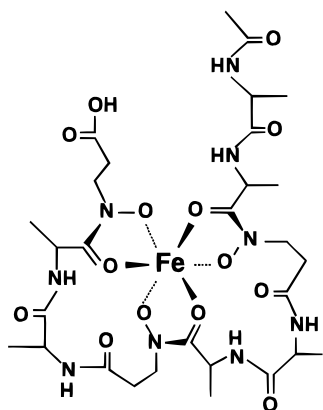


Figure 6. Structure of Fe(III)-1 shown in the Δ -*C-cis,cis* configuration. A similar Δ -*C-cis,cis* configuration is assigned to the structure of Fe(III)-2. For nomenclature, see footnote 41.

complexes ferrichrome and coprogen.^{35,36} These negative and positive spectral patterns have been assigned to the Δ configuration around the metal ion with reference to the literature assignment.^{35,37} These CD spectra may be correlated with the ligand structure; in a suitably constrained sequence, the methyl group of the L-Ala-NO⁻ moiety perhaps forces an iron complex to take the Δ configuration with a sharp twist, so as to avoid the overlap with β -hydrogens in the CO-N(O⁻)CH₂CH₂CO-residue.

For the octahedral iron(III) complexes of a linear trihydroxamate, there are eight theoretically possible isomers of the Δ configuration.³⁸ These are *C-cis,cis*; *C-cis,trans*; *C-trans,cis*; *C-trans,trans*; and four similar versions for the *N*-series, when they are designated^{5,39,40} according to a Raymond type nomenclature.⁴¹ Examination of CPK molecular models for Fe(III)-1 reveals that all the hydroxamate groups must be placed in the same orientation (*cis* orientation) with respect to the metal ion in order to maintain an octahedral arrangement; introduction of any *trans*-oriented hydroxamate group fails to retain the octahedral arrangement because of the strain of the sequence. Of the two *cis,cis* arrangements, the *N-cis,cis* must be abandoned, because it requires a detoured chain bridging between the hydroxamate groups of the nearest neighbor. Thus, the only possible configuration, assignable to Fe(III)-1, is the Δ -*C-cis,cis* (Figure 6). As for Fe(III)-2, it has the same sequence and shows the same CD pattern as that of Fe(III)-1; accordingly, its configuration is also assigned to Δ -*C-cis,cis*. These exclusive assignments are strongly supported by the observed large CD intensities.

In order to investigate the structure of the iron(III) complexes by ¹H NMR spectroscopy, we attempted formation of diamag-

netic complexes with Al(III) or Ga(III), in expectation that they would have the same coordination geometry as that of the iron(III) complexes. However, the insolubility of the formed complexes precluded the NMR study.

Unlike the present ligands, desferrioxamines are flexible.² They lack chiral centers and tend to produce iron(III) complexes of different optical and geometrical isomers, as demonstrated by the preparation of chromium(III) desferrioxamine B.³⁹ From an NMR study of the gallium desferrioxamine B complex, Borgias et al. indicated that there are two significant isomers in solution, most likely the *N-cis,cis* and *C-trans,trans* isomers, regardless of the chirality.⁴² The *N-cis,cis* configuration corresponds to the *C-cis,cis* of the present complex, since the direction of the hydroxamate group is reversed in desferrioxamines. The *N-trans,trans* isomer is unlikely for the present ligands, as discussed above. Thus, these results suggest that suitable constraint of a chiral ligand favors formation of iron(III) complexes with well-defined structures.

Note that Shanzer's group synthesized α -amino acid-based trihydroxamates using the β (HO)Ala unit and examined their iron(III)-holding properties.¹⁶ The most successful ligands contained the glutamic acid unit and had the sequence of a seven-atom spacing with one amide bond. The iron-exchange kinetics study was performed in aqueous 80% MeOH with cyclohexylene-1,2-dinitrilotetraacetate. Because of the difference in experimental conditions, it is difficult to compare our data with theirs, although it appears that both their seven-atom spacing and our eight-atom spacing with two amide bonds seem to afford useful chiral ligands.

Conclusions. The preparation of a pair of linear and cyclic peptide-based ligands (1 and 2) is useful for examining the features of a unit sequence and the ligands obtained. By addition of three methylene units to the nonapeptide reported previously,¹⁸ the ligands become much less strained but still have constraint relative to desferrioxamines. Characterization of the linear and cyclic pair ligands allows us to better understand the iron(III)-holding behavior of the peptide-based chelators. For example, the complex formed from the linear ligand, Fe(III)-1, is more resistant to H⁺ or OH⁻ attack than Fe(III)-2, whereas Fe(III)-2 holds iron(III) more tightly than Fe(III)-1 in the metal-exchange reaction. The rate-determining step of this exchange reaction is proposed to occur at the dissociation step of the second hydroxamate group. Protonation equilibrium and iron(III)-exchange kinetics show that Fe(III)-1 and Fe(III)-2 are less stable and more labile than ferrioxamine B, although the magnitudes of their stability constants are nearly comparable to those of the ferrioxamines. Most importantly, the ligands made from the Ala-Ala- β (HO)Ala sequence produce chiral iron(III) complexes of well-defined structure.

Experimental Section

General Procedures. The melting points are uncorrected. IR spectra were recorded on a JASCO Model A-302 spectrophotometer, and UV-vis spectra were obtained on a Hitachi 320A spectrophotometer. CD spectra were taken with a JASCO J-40 spectrophotometer. HPLC was carried out on a JASCO 880-PU apparatus combined with 875-UV and 100-III attachments, using a column (4.6 \times 250 mm) of Finepac SIL C₁₈. A solvent system of CH₃CN-H₂O (3:1 v/v) containing 0.1% phosphoric acid was applied at a flow rate of 1 cm³/min and the retention time (*R_t*) was determined. For GPC a column (7.8 \times 300 mm) of TSK-GEL G2000 HHR was used with EtOH as solvent. Optical rotations were measured with a Horiba SWPA-2000 polarimeter at 25 $^{\circ}$ C. ¹H NMR spectroscopy was carried out in CDCl₃ or DMSO-*d*₆ with a JEOL FX-200 or a GX-270 spectrometer using

(35) van der Helm, D.; Baker, J. R.; Eng-Wilmont, D. L.; Hossain, M. B.; Loghry, R. A. *J. Am. Chem. Soc.* **1980**, *102*, 4224.

(36) Wong, G. B.; Kappel, M. J.; Raymond, K. N.; Matzkanke, B.; Winkelmann, G. *J. Am. Chem. Soc.* **1983**, *105*, 810.

(37) Zalkin, A.; Forrester, J. D.; Templeton, D. H. *J. Am. Chem. Soc.* **1966**, *88*, 1810.

(38) Bickel, H.; Hall, G. E.; Keller-Schierlein, W.; Prelog, V.; Vischer, E.; Wettstein, A. *Helv. Chim. Acta* **1960**, *43*, 2129.

(39) Leong, J.; Raymond, K. N. *J. Am. Chem. Soc.* **1975**, *97*, 293.

(40) Müller, G.; Raymond, K. N. *J. Bacteriol.* **1984**, *160*, 304.

(41) The isomers are named as follows:⁵ Viewed down the pseudo-C₃ axis, Δ isomers have a right-handed propeller configuration around the metal ion. The sequence of each hydroxamate group (ring 1, 2, or 3) corresponds to the rotation direction, beginning with the nearest N-terminal hydroxamate chelation (ring 1). When ring 1 has the carbon atom of the hydroxamate group above the nitrogen, it is denoted "*C*". Each of rings 2 and 3 is called *cis* or *trans* depending upon whether it has the same or opposite orientation relative to ring 1. This is the same rule that Leong et al. proposed originally,³⁹ but the structures are depicted as seen downward from up rather than upward from down. The previous iron(III) nonapeptide¹⁸ should be called Δ -*C-cis,cis* instead of *N-cis,cis*.

(42) Borgias, B.; Hugi, A. D.; Raymond, K. N. *Inorg. Chem.* **1989**, *28*, 3538.

Me₄Si as the standard. Double-distilled water was deionized by passing through an ion-exchange resin (Dowex 50W-X8).

Boc-Ala-β(BnO)Ala-Ome. To a solution of Boc-Ala-OH (19.9 g, 105 mmol) and triethylamine (14.7 cm³, 105 mmol) in THF (500 cm³) were added dropwise a solution of isobutyl chloroformate (13.8 cm³, 105 mmol) in THF (50 cm³) at -15 °C and then a solution of β(BnO)-Ala-Ome¹³ (20.9 g, 100 mmol) in THF (50 cm³). The mixture was stirred for 3 h at -15 °C, stored in a refrigerator for 48 h, and filtered. The filtrate was evaporated; the residue was dissolved in EtOAc (500 cm³), washed with 5% NaHCO₃, 5% citric acid, and brine, and then dried (MgSO₄). Evaporation of the solvent gave an oily product (40 g, 95%), which was directly used further: HPLC *R_f*, 4.6 min; IR (film, cm⁻¹) 1740 (C=O, ester), 1705 (C=O, urethane), 1670 (C=O, amide); ¹H NMR (CDCl₃) δ 1.28 (3H, d, *J* = 7.1 Hz, Me), 1.45 (9H, s, *t*-Bu), 2.58 (2H, t, *J* = 7.0 Hz, CH₂CO), 3.60 (3H, s, OMe), 3.7–4.2 (2H, m, NCH₂), 4.72 (1H, m, α-CH), 4.94 (2H, m, PhCH₂), 5.38 (1H, br s, NH), 7.40 (5H, m, Ph).

Boc-Ala-Ala-β(BnO)Ala-Ome (3a). Boc-Ala-β(BnO)Ala-Ome (2.82 g, 7.41 mmol) was treated with 8.6 mol dm⁻³ HCl/dioxane (18 cm³) for 40 min at 0 °C and evaporated to give a residue. The residue, Boc-Ala-OH (1.58 g, 8.36 mmol), NMM (0.868 cm³, 7.89 mmol), HOBt (1.53 g, 10.0 mmol), and EDC·HCl (1.92 g, 10.0 mmol) were dissolved in CH₂Cl₂ (20 cm³) at -10 °C, and the resulting solution was stirred for 3 h at -10 °C and for 24 h at room temperature, and then evaporated to yield an oil. The oil was dissolved in EtOAc (100 cm³) and washed with 5% NaHCO₃, 5% citric acid, and brine, and then dried (MgSO₄) and evaporated to give a product, which was recrystallized as colorless needles (2.58 g, 75%): mp 110–111 °C (from hexane–EtOAc); IR (KBr, cm⁻¹) 1740, 1700, 1650 (amide); ¹H NMR (CDCl₃) δ 1.30 (3H, d, *J* = 6.8 Hz), 1.36 (3H, d, *J* = 6.8 Hz), 1.45 (9H, s), 2.58 (2H, t, *J* = 6.7 Hz), 3.62 (3H, s), 3.7–4.2 (2H, m), 4.23 (1H, m, α-CH), 4.93 (2H, s, PhCH₂), 4.98 (1H, m, α-CH), 5.05 (1H, br s, Boc-NH), 6.78 (1H, br d, NH), 7.40 (5H, m).

Boc-Ala-Ala-β(BnO)Ala-OH (3b). Compound 3a (14.6 g, 32.3 mmol) in MeOH (250 cm³) was stirred with aqueous NaOH (1 mol dm⁻³; 42 cm³) at room temperature for 2.5 h. The solution was treated with 30% citric acid (42 cm³) and evaporated. A residue was extracted with CHCl₃ (100 cm³ × 3), dried (MgSO₄), and then evaporated to give a solid product (15.5 g, ca. 100%): HPLC *R_f*, 3.0 min; IR (KBr, cm⁻¹) 1710, 1650; ¹H NMR (CDCl₃) δ 1.28 (2H, d, *J* = 7.1 Hz), 1.34 (3H, d, *J* = 7.1 Hz), 1.44 (9H, s), 2.61 (2H, t, *J* = 6.6 Hz), 3.7–4.2 (2H, m), 4.22 (1H, m), 4.95 (2H, s), 5.00 (1H, m), 5.28 (1H, br s), 7.11 (1H, br d), 7.40 (5H, m).

Boc-[Ala-Ala-β(BnO)Ala]₂-Ome (4). The Boc group of 3a (6.59 g, 14.6 mmol) was removed with 8.6 mol dm⁻³ HCl/dioxane (32 cm³) to yield an amino derivative, which was condensed with 3b (7.03 g, 21.9 mmol) by the use of EDC·HCl and HOBt. A product (12.5 g) was obtained almost quantitatively, which was directly used further: HPLC *R_f*, 3.8 min; IR (KBr, cm⁻¹) 1730, 1700, 1650; ¹H NMR (CDCl₃) δ 1.24 (3H, d, *J* = 6.8 Hz), 1.27 (6H, d, *J* = 7.1 Hz), 1.33 (3H, d, *J* = 7.1 Hz), 1.44 (9H, s), 2.54 (4H, m, 2 × CH₂CO), 3.61 (3H, s), 3.7–4.2 (4H, m, 2 × NCH₂), 4.22 (1H, m, α-CH), 4.50 (1H, q, *J* = 7.0 Hz, α-CH), 4.92 (2H, s), 4.94 (2H, s), 4.97 (2H, m, α-CH), 5.24 (1H, br s), 6.78 (1H, br d), 7.02 (1H, br d), 7.08 (1H, br d), 7.39 (10H, m).

Boc-[Ala-Ala-β(BnO)Ala]₃-Ome (5). This was obtained from 4 (12.5 g) and 3b (7.0 g) by a similar procedure for 4 and purified by column chromatography on silica gel with CHCl₃–MeOH (10:1) as the eluent to yield a product (13.6 g, 85%): HPLC *R_f*, 3.8 min; IR (KBr, cm⁻¹) 1735, 1700, 1640; ¹H NMR (CDCl₃) δ 1.24 (6H, d, *J* = 7.0 Hz, 2 × Me), 1.27 (9H, d, *J* = 7.1 Hz, 3 × Me), 1.31 (3H, d, *J* = 7.0 Hz, Me), 1.43 (9H, s), 2.54 (6H, m, 3 × CH₂CO), 3.60 (3H, s), 3.7–4.2 (6H, m, 3 × NCH₂), 4.25 (1H, m, α-CH), 4.55 (2H, m, 2 × α-CH), 4.91 (6H, s, 3 × PhCH₂), 4.98 (3H, m, 3 × α-CH), 5.27 (1H, d, *J* = 7.0 Hz, NH), 6.80 (1H, br, NH), 6.95 (1H, br, NH), 7.05 (1H, br, NH), 7.20 (1H, br, NH), 7.38 (15H, m, 3 × Ph), 7.40 (1H, br, NH).

Ac-[Ala-Ala-β(HO)Ala]₃-OH (1). Compound 5 (1.0 g, 0.92 mmol) was treated with TFA (15 cm³, 200 mmol) in CH₂Cl₂ (5 cm³) for 2 h at 0 °C, then acylated with *N*-acetoxy succinimide (0.32 g, 2.0 mmol),⁴³ and purified by column chromatography on silica gel with CHCl₃–MeOH (10:1) as the eluent to give Ac-[Ala-Ala-β(BnO)Ala]₃-Ome (0.60 g, 63%): IR (KBr, cm⁻¹) 1735, 1650. Ac-[Ala-Ala-β(BnO)-

Ala]₃-Ome (0.276 g, 0.267 mmol) in MeOH (5 cm³) was treated with aqueous NaOH (1 M; 0.4 cm³) similarly to the case of 3b, to provide Ac-[Ala-Ala-β(BnO)Ala]₃-OH as a solid (0.269 g, 99%): HPLC *R_f*, 3.3 min; IR (KBr, cm⁻¹) 2550, 1720 (CO₂H), 1640. Ac-[Ala-Ala-β(BnO)Ala]₃-OH (0.14 g, 0.14 mmol) in MeOH (100 cm³) was hydrogenated with H₂ in the presence of palladium(II) acetate (3.3 mg) for 20 h. The catalyst was removed by filtration. Evaporation of the solvent, followed by purification with a Sephadex G-15 column, gave a product as a white solid (75 mg, 75%): HPLC *R_f*, 2.7 min. Anal. Calcd for C₂₉H₄₉N₉O₁₄·²/₃H₂O: C, 45.85; H, 6.68; N, 16.59. Found: C, 45.83; H, 6.51; N, 16.46. Optical rotation: [α]_D²⁵ -25° (*c* 0.2 in DMSO). IR (KBr, cm⁻¹): 3260 (NOH), 1680, 1650, 1620 (CONOH).

Cyclo-[Ala-Ala-β(HO)Ala]₃ (2). Compound 4 (1.09 g, 1.00 mmol) in MeOH (10 cm³) was hydrolyzed to give Boc-[Ala-Ala-β(BnO)Ala]₃-OH (ca. 100%): HPLC *R_f*, 3.0 min. Boc-[Ala-Ala-β(BnO)Ala]₃-OH (0.54 g, 0.50 mmol) was treated with TFA (4 cm³, 50 mmol) in CH₂Cl₂ (1 cm³) for 2.5 h at 0 °C and evaporated to yield a residue. The residue was dissolved in DMF (500 cm³), and the solution was neutralized (pH 6.5) with triethylamine (1.1 cm³). The BOP reagent (0.44 g, 1.0 mmol) and HOBt (0.16 g, 1.0 mmol) were added at -10 °C, and the mixture was stirred for 4 h at 0 °C and 2 d at room temperature. The solvent was removed under reduced pressure, and the residue was dissolved in CHCl₃ (100 cm³), washed with 5% NaHCO₃ and 5% citric acid, and then dried (MgSO₄). Purification with column chromatography on silica gel with CHCl₃–MeOH (8:1/v) as the eluent gave cyclo-[Ala-Ala-β(BnO)Ala]₃ in 31% yield (0.15 g): GPC *R_f*, 30.1 min, which corresponded to a molecular weight of 1 × 10³, nearly equal to a calculated value of 958 for the monocyclusation product; IR (KBr, cm⁻¹) 1650 (amide); ¹H NMR (CDCl₃) δ 1.07 (9H, d, *J* = 6.6 Hz, 3 × Me), 1.27 (9H, d, *J* = 6.8 Hz, 3 × Me), 2.50 (6H, m), 3.60–4.40 (6H, m), 4.51 (3H, m), 4.82 (3H, m), 4.86 (6H, s), 6.78 (3H, br s), 7.38 (15H, m), 7.75 (3H, br s). Cyclo-[Ala-Ala-β(BnO)Ala]₃ (100 mg, 0.104 mmol) was hydrogenated with H₂ in the presence of Pd–C (10%; 10 mg) in MeOH (50 cm³), and workup similar to 1 afforded a product as a white solid (79 mg, 75%): HPLC *R_f*, 3.3 min. Anal. Calcd for C₂₇H₄₅N₉O₁₂·¹/₂H₂O: C, 46.55; H, 6.65; N, 18.09. Found: C, 46.61; H, 6.60; N, 18.06. Optical rotation: [α]_D²⁵ +20° (*c* 0.3 in DMSO). IR (KBr, cm⁻¹): 3320 (NOH), 1640 (CO amide).

Determination of pK's. Potentiometric titrations were performed under an argon atmosphere to ensure the absence of O₂ and CO₂, using an autoburet (Toa Electronics ABT-101) equipped with a titration flask maintained at 25.0 ± 0.1 °C and with a Toa Electronics GST-5311C combined electrode, which consists of an Ag–AgCl electrode, a reference electrode, and a thermal electrode compensator. The glass electrode was adjusted at three pH values (pH 4.01, 6.86, and 9.18) with standard buffer solutions as defined by the Japanese Industrial Standard (JIS Z 8802). The electrode system was calibrated to obtain a hydrogen ion concentration from a pH-meter reading by titrating known amounts of HCl with CO₂-free NaOH solution in low-pH and high-pH regions and by determining the junction potentials.⁴⁴ A ligand (2.0 × 10⁻⁵ mol) was dissolved in degassed, deionized water (20.0 cm³), and the ionic strength was maintained constant with KCl (0.01). A carbonate-free NaOH solution (0.1 mol dm⁻³), which was prepared from Merck Suprapur NaOH·H₂O, was fed automatically through a syringe, and both the amount of NaOH and pH of the solution were recorded consecutively. The trace amount of CO₂ in the NaOH solution was calibrated by a Gran's plot.⁴⁵ For the pK determinations, titrations were carried out over ranges of pH 4.6–10.2 for ligand 1 and pH 4.8–10.6 for ligand 2 at ca. 100 determination points. On the basis of these data, the pK's of ligands 1 and 2 were calculated using the program PKAS, with σ < 1.0.²⁷ The pK value was an average of at least two determinations with an error limit of ±0.05 pK unit. This procedure was also checked by reproducing those values reported²⁶ for desferrioxamine B.

Iron(III) Complex Formation. (a) A stock solution of ferric nitrate (2.93 × 10⁻³ mol dm⁻³) was prepared, and its concentration was determined by the bismuth method with EDTA. In a 10 mm cell held at a constant temperature of 25.0 ± 0.1 °C in the cell compartment of a Hitachi spectrometer, a ligand (7.82 × 10⁻⁷ mol) and a KNO₃ solution

(44) Irving, H. M.; Miles, M. G.; Pettit, L. D. *Anal. Chim. Acta* **1967**, *38*, 475.

(45) Gran, G. *Analyst* **1952**, *77*, 661.

(43) Lindsay, D. G.; Shall, S. *Biochem. J.* **1971**, *121*, 737.

(1 mol dm⁻³; 0.30 cm³) were placed and diluted with water (2.43 cm³). To this was added an iron(III) solution (0.267 cm³, 7.82 × 10⁻⁷ mol). The pH of the solution was determined (pH 2.1). The solution of pH 2.1 was neutralized with 0.1 mol dm⁻³ KOH to give a solution of pH 7.0, and the CD spectrum was determined.

(b) UV-vis spectra were recorded for iron(III) complex solutions of different pH values. These solutions were obtained by a serial addition of a small amount of either 0.1 mol dm⁻³ HNO₃ or 0.1 mol dm⁻³ KOH solution to an iron(III) complex solution of pH 7.0.

(c) A Schwarzenbach plot was made using the data from solutions that exhibited an isosbestic point in their UV-vis spectra during serial acidification of a neutral solution of an iron(III) complex.

Rates of Iron(III) Exchange with EDTA. The above prepared iron(III) complex solution of pH 2.1 (1.42 cm³, 2.60 mmol) was diluted with a buffer solution (1.42 cm³) of ionic strength of 0.1 (KCl) in a 10 mm cell. The solution was kept in the cell compartment held at 25.0 °C. To initiate an exchange reaction, a solution of EDTA (0.1 mol dm⁻³; 0.156 cm³) was added, and a decrease in the absorbance at 425 nm was monitored with time. A pseudo-first-order rate constant was obtained from a plot of the absorbance vs time; most of these plots conformed to the first-order reaction rate up to 80% conversion. The observed rate (*k*_{obs}) was obtained as an average value at least two determinations with error limits of ±5% for pH 5.4 and ±10% for pH 2.1. Buffer solutions were prepared from the following acid-base combinations dissolved in water with KCl: Tris-HCl (pH 7.0), acetic acid-NaOH (pH 5.4), and glycine-HCl (pH 2.1).

Equilibrium Competition Reaction with EDTA. To an iron(III) complex solution prepared as above in a cell (2.6 × 10⁻⁴ mol dm⁻³; 2.90 cm³) was added a solution of EDTA (0.01 mol dm⁻³; 0.078 cm³) at a given pH, and the progress of the exchange reaction was followed by monitoring a decrease in the absorbance at 425 nm, while a constant temperature of 25.0 °C was maintained. The pH of the solution was adjusted by addition of a small amount of KOH solution, when it was necessary. Several days were usually required to attain an equilibrium of the reaction. After determination of the iron(III) complex concentration in the solution, the equilibrium quotient (*K*_{eq} value) was calculated from the concentrations of species involved, that is, the ligand, Fe(III)-ligand, EDTA, and Fe(III)-EDTA, and these concentrations were calculated on the basis of the stoichiometry of the reaction and their protonation constants: [Fe(L)] + [Fe(EDTA)]⁻_{total} = 2.6 × 10⁻⁴ mol dm⁻³, [EDTA]_{total} + [H₃L]_{total} = 2.6 × 10⁻⁴ mol dm⁻³, [Fe(EDTA)]⁻ = [Fe(EDTA)]⁻_{total} / {1 + 1/([H⁺]K_{OH^{edta}})} where K_{OH^{edta}} = 10^{7.43}, [H₃L] = [H₃L]_{total} / {1 + 1/([H⁺]K₃) + 1/([H⁺]²K₂K₃) + 1/([H⁺]³K₁K₂K₃)}, and [H₂EDTA²⁻] = [EDTA]_{total} / {K_{3^{edta}}K_{4^{edta}}[H⁺]² + K_{3^{edta}}[H⁺] + 1 + 1/(K_{2^{edta}}[H⁺] + 1/(K_{1^{edta}}K_{2^{edta}}[H⁺]²))}.}

Acknowledgment. We thank Yukio Shirozume for his efforts in the initial stage of the study and Dr. J. M. Pope for reading the manuscript.

IC951338A